Studies with Chimeras of the Gonadotropin Receptors Reveal the Importance of Third Intracellular Loop Threonines on the Formation of the Receptor/Nonvisual Arrestin Complex†

Ravi Sankar Bhaskaran, Le Min, Hanumanthappa Krishnamurthy, and Mario Ascoli*

Department of Pharmacology, The University of Iowa, Iowa City, Iowa 52246

Received May 28, 2003; Revised Manuscript Received August 14, 2003

ABSTRACT: Using chimeras and more discrete exchange mutations of the rat (r) and human (h) gonadotropin receptors, we had previously identified multiple noncontiguous residues of the lutropin (LHR) and follitropin (FSHR) receptors that dictate their rates of internalization. Since the internalization of the LHR and the FSHR is driven by their abilities to associate with the nonvisual arrestins, we hypothesized that one or more of the residues previously identified by the internalization assays are involved in the formation of the receptor/nonvisual arrestin complex. In the studies reported herein, we tested this hypothesis by measuring the association of arrestin-3 with a large number of rLHR/hLHR and rFSHR/hFSHR exchange mutants that affect internalization. The results presented show that the same residues that dictate the rate of internalization of these two receptor pairs affect their ability to associate with arrestin-3. Although these residues are located in distinct topological domains, our analyses show that threonine residues in the third intracellular loop of both receptor pairs are particularly important for the formation of the receptor/arrestin-3 complexes and internalization. We conclude that the different rates of internalization of the gonadotropin receptors are dictated by their different abilities to associate with the nonvisual arrestins and that this association is, in turn, largely dictated by the presence of threonine residues in their third intracellular loops.

Although much has been recently learned about the role of the nonvisual arrestins in the trafficking of G protein-coupled receptors (GPCRs)[1] (*1*−*5*), there is a relative paucity of information on the identity of specific GPCR residues that participate in GPCR trafficking and nonvisual arrestin binding.

In an attempt to define structural features of GPCRs that participate in trafficking, we (*6*−*9*) and others (*10*) have taken advantage of differences in the rates of internalization and postendocytotic fates and the high degree of amino acid sequence identity displayed by the glycoprotein hormone receptors to identify residues that influence these processes. For example, studies utilizing chimeras of the lutropin (LHR) and thyrotropin (TSHR) receptors as well as chimeras of the hLHR and rLHR have shown that the serpentine and/or intracellular domains of these receptors contain structural features that determine their routing to the recycling vs the degradation pathways (*9*−*11*). Other studies on LHR/TSHR and LHR/FSHR chimeras have also shown that their extracellular domains play a role in the rate and/or the extent of internalization (*6*, *10*). In more recent studies we have systematically analyzed chimeras and exchange mutants of the gonadotropin receptors from two different species, the hLHR and rLHR or the hFSHR and the rFSHR, to identify several noncontiguous, intracellular residues that dictate the rate of internalization of these receptors (*7*, *8*). The identified residues are located in the C-terminal tail, transmembrane regions 4 and 7 (TM4 and TM7), and intracellular loops 2 and 3 (iL2 and iL3). Interestingly, the only region that is common to the two receptors is the third intracellular loop (*7*, *8*).

Since the internalization of the gonadotropin receptors is driven by their interactions with the nonvisual arrestins (*7*, *8*), we hypothesized that the residues identified as being required for internalization could be involved in the binding of the nonvisual arrestins. Using a recently described cotransfection assay that can be used to measure the association of the nonvisual arrestins with GPCRs (*12*−*14*), we now show that this hypothesis is indeed correct. We also present additional mutagenesis studies on discrete amino acid residues present in the third intracellular loop that modulate the association of the gonadotropin receptors with the nonvisual arrestins and their rates of internalization.

MATERIALS AND METHODS

Plasmids. Expression vectors for the rat and human gonadotropin receptors and mutants thereof were as described (*7*, *8*). All receptors were modified to express the myc epitope at their N-terminus as described elsewhere (*15*, *16*). The new

† This work was supported by Grants from the National Institutes of Health (CA-40629 and HD-28962) to M.A.

* Address correspondence to this author at the Department of Pharmacology, 2-319B BSB, 51 Newton Rd., The University of Iowa, Iowa City, IA 52242-1109. Phone 319-335-9907; fax 319-335-8930; e-mail mario-ascoli@uiowa.edu.

[1] Abbreviations: LHR, lutropin receptor; FSHR, follitropin receptor; TSHR, thyrotropin receptor; CG, chorionic gonadotropin; FSH, follitropin; GPCR, G protein-coupled receptor; TM, transmembrane; iL, intracellular loop; prefixes h and r, human and rat, respectively; Hepes, *N*-(2-hydroxyethyl)piperazine-*N*′-2-ethanesulfonic acid; Tris, tris(hydroxymethyl)aminomethane; EDTA, ethylenediaminetetraacetic acid; SDS, sodium dodecyl sulfate; PVDF, poly(vinylidene difluoride).

10.1021/bi034907w CCC: $25.00
Published on Web 10/30/2003

mutants described here were prepared by use of a site-directed mutagenesis kit from Stratagene with the myc epitope-tagged receptors as templates. An expression vector for arrestin-3 was initially provided by Dr. Jeff Benovic (Thomas Jefferson University, Philadephia, PA) and it was modified to express the FLAG epitope at the N-terminus (*12*). HA-tagged dynamin K44A (*17*) was kindly provided by Dr. Sandra Schmid (Scripps Research Institute, La Jolla, CA).

Measurement of the Association of the Gonadotropin Receptors with the Arrestin-3 in Cotransfected Cells. 293T cells were maintained in Dulbecco's modified Eagle's medium containing 10 mM Hepes, 10% newborn calf serum, and 50 μg/mL gentamicin, pH 7.4. Transient transfections were done by the calcium phosphate method of Chen and Okayama (*18*). Cells were plated in gelatin-coated 100-mm dishes and transfected when 70−80% confluent with the myc-tagged receptors (5 μg), FLAG-arrrestin-3 (0.5 μg), and HA-dynamin-K44A (2.5 μg). After an overnight incubation, the cells were washed and used 24 h later.

The association of the receptors with arrestin-3 was measured in cotransfected cells as described in detail elsewhere (*12*−*14*). Briefly, the monolayers were washed three times and the cells were incubated with vehicle only or with a saturating concentration of hCG or hFSH (25−50 nM) for 30 min at 37 °C. At the end of this incubation the cells were cross-linked with 1.5 mM DSP [dithiobis-(succinimidopropionate)] for 30 min at room temperature while the dishes were rocked. The cross-linked cells were washed and lysed as described before (*12*, *13*) except that RIPA buffer (150 mM NaCl, 50 mM Tris, 1 mM EDTA, 1% NP-40, 0.5% sodium deoxycholate, and 0.1% SDS, pH 7.4) was used instead of the previously described lysis buffers. The lysates were clarified by centrifugation, and aliquots (∼500 μL) containing the same amount of protein were immunoprecipitated with a monoclonal antibody to the myc epitope (9E10) that had been preabsorbed to agarose-conjugated protein G overnight at 4 °C as described previously (*16*). After extensive washing, the cross-linked complexes were reduced and eluted by vigorous mixing of the beads in SDS sample buffer with reducing agents for 15 min at room temperature. The eluted material was then resolved on SDS gels and electrophoretically transferred to PVDF membranes as described elsewhere (*19*).

FLAG-arrestin-3 and the myc-tagged receptors were detected in blots of the immunoprecipitates or lysates by use of an anti-FLAG (M2) monoclonal antibody covalently coupled to horseradish peroxidase (final dilution of 1:500) or an anti-myc (9E10) monoclonal antibody covalently coupled to horseradish peroxidase (final dilution of 1:1000). All immune complexes were ultimately visualized and quantitated by use of the Super Signal West Femto Maximum Sensitivity system of detection from Pierce and a Kodak digital imaging system. This image capture system is set up to alert us when image saturation occurs and to prevent us from measuring the intensity of such images.

Hormone Internalization Assays. 293T cells were plated in 100-mm dishes and transfected with the desired receptor constructs (5 μg) alone (Tables 1 and 2) or together with increasing amounts of FLAG-arrestin-3 (Figure 6) by the method described above. At the end of the transfection the cells were washed, trypsinized, and plated in gelatin-coated 35-mm wells and used 24 h later for internalization assays.

Determinations of the rates of internalization (Tables 1 and 2) were done with at least five different data points collected at 3−10 min intervals (depending on the construct transfected) after the addition of a subsaturating (∼2 nM) concentration of ^{125}I-hFSH or ^{125}I-hCG. The endocytotic rate constant (k_e) was calculated from the slope of the line obtained by plotting the ratio of internalized to surface-bound hormone against time or by plotting the internalized radioactivity against the integral of the surface-bound radioactivity (*6*, *20*−*23*). The half-time of internalization ($t_{1/2}$) is defined as $0.693/k_e$.

Single-point internalization assays such as those shown in Figure 6 were done with the same hormone concentrations listed above, but a single 10 min incubation was used and the results were expressed as the ratio of internalized/surface-bound hormone.

Other Methods. Hormonal responsiveness was assessed by measuring cAMP accumulation in transiently transfected cells plated in gelatin-coated 35-mm wells. Total cAMP was measured as described elsewhere (*13*) at the end of a 2 h incubation (37 °C) with increasing concentrations of hCG or hFSH. Plots of the dose−response curves were drawn by fitting the data obtained to a sigmoidal equation with the Prism software package from GraphPad Software Inc.

Statistical analyses (*t*-test) were performed with the InStat software package from GraphPad Software Inc.

Hormones and Supplies. Human kidney 293T cells are a derivative of 293 cells that express the SV40T antigen (*24*) and were provided to us by Dr. Marlene Hosey (Northwestern University, Chicago, IL). The 9E10 hybridoma cell line was obtained from the American Type Culture Collection. Purified hCG (CR-127, ∼13 000 IU/mg) and purified hFSH were purchased from Dr. A. Parlow and the National Hormone and Pituitary Agency of the National Institute of Diabetes and Digestive and Kidney Diseases. Purified recombinant hFSH and hCG[2] were provided by Ares Serono (Randolph, MA). Cell culture medium was obtained from the Media and Cell Production Core of the Diabetes and Endocrinology Research Center of the University of Iowa. Concentrated supernatant from the 9E10 cells was prepared by the Hybridoma Facility of the Cancer Center of the University of Iowa. The 9E10 and anti-FLAG M2 monoclonal antibodies coupled to horseradish peroxidase were purchased from Boehringer Mannheim and Sigma, respectively. Other cell culture supplies, plasticware, and reagents were obtained from Corning and Gibco. All other chemicals were obtained from commonly used suppliers.

RESULTS

We have recently devised an approach that exploits the high degree of amino acid sequence identity of the rat and human gonadotropin receptors and their divergent rates of internalization to identify the intracellular residues of these receptors that participate in agonist-induced internalization (*7*, *8*). The residues so identified are highlighted in Figure 1. The residues highlighted with darker shading on the top two lines are responsible for the different half-times of internalization of hCG mediated by the rLHR and hLHR,

[2] Both preparations were used in this study and were found to be indistinguishable.

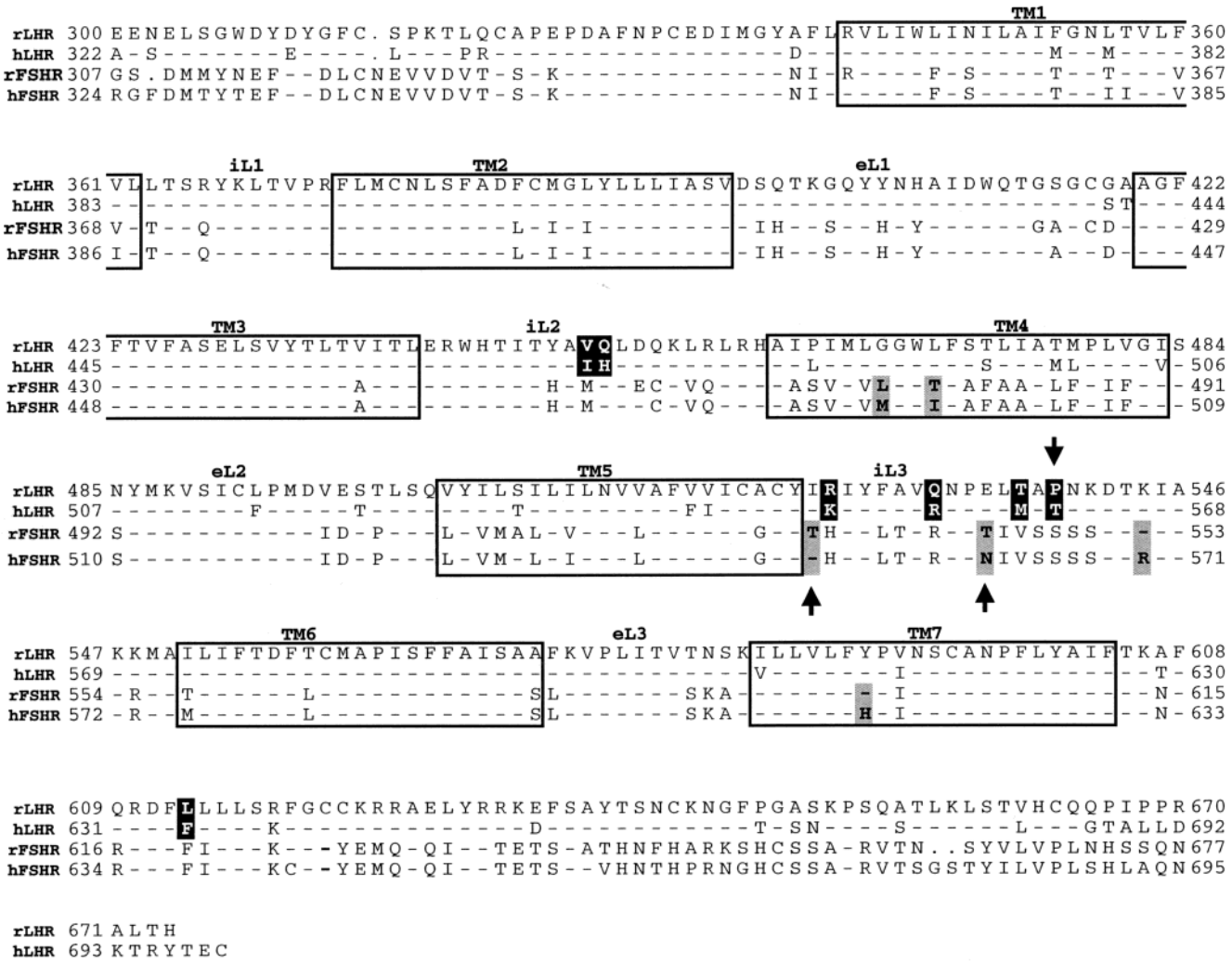

FIGURE 1: Amino acid sequence alignment of the rat and human gonadotropin receptors. The amino acid sequences of the rFSHR, hFSHR, rLHR, and hLHR were taken from refs *39*, *40*, *41*, and *42*, respectively. The amino acid sequence of the C-terminal half of the rLHR is shown in the single-letter code. A dash under a given rLHR residue indicates that the corresponding residue in the other receptor is identical to that of the rLHR. Residues that are not identical to those of the rLHR are identified with the appropriate single-letter code. Dots indicate gaps introduced for optimal alignment. The seven transmembrane regions are labeled TM1−TM7, and the three intracellular and extracellular loops are labeled iL1−iL3 and eL1−eL3, respectively. The seven noncontiguous residues present in the serpentine and C-terminal domains that were previously shown to dictate the rate of internalization of the LHR (see ref *7*) are highlighted (darker shading), and the six noncontiguous residues present in the serpentine region that were shown here to dictate the rate of internalization of the FSHR (see ref *8*) are also highlighted (lighter shading). The third intracellular loop residues identified here as being involved in arrestin-3 binding are marked with arrows.

and those highlighted with lighter shading in the bottom two lines are responsible for the different half-times of internalization of hFSH mediated by the rFSHR and the hFSHR.

To determine if these residues modulate the association of the gonadotropin receptors with the nonvisual arrestins, we used an approach described recently to measure the association of different GPCRs with arrestin-3 in intact cells (*12*−*14*, *25*). In our version of this approach, 293T cells are cotransfected with a mixture of a myc-tagged receptor, FLAG-tagged arrestin-3, and dynamin-K44A and the formation of the receptor/arrestin-3 complex is measured by probing anti-myc immunoprecipitates of cross-linked cells with anti-myc and anti-FLAG antibodies (*12*−*14*). Since cotransfection with dynamin-K44A prevents the internalization of the receptor/nonvisual arrestin complexes, this cotransfection approach allows for the measurement of the formation of the receptor/arrestin complexes at the cell surface and independently of their different rates of internalization (*12*−*14*). By this approach, an increase in receptor-associated arrestin-3 can be readily detected in cells cotransfected with a constant amount of receptor and increasing amounts of arrestin-3 but the formation of the complex is, as expected, a saturable phenomenon (*12*, *14*). When 293T cells plated in 100-mm dishes are cotransfected with 5 μg of the myc-hLHR, 2.5 μg of dynamin-K44A, and increasing amounts of FLAG-arrestin-3, half-maximal saturation of the hLHR/arrestin-3 complex is attained in cells cotransfected with ~1 μg of FLAG-arrestin-3/100-mm dish (*12*). Under the same conditions, cells cotransfected with 5 μg of the myc-rFSHR, 2.5 μg of dynamin-K44A, and increasing amounts of FLAG-arrestin-3 display half-maximal saturation when cotransfected with ~2 μg of FLAG-arrestin-3/100-mm dish (*14*).

In the experiments described below we always measured the formation of the arrestin-3/receptor complex with 293T cells plated in 100-mm dishes and cotransfected with 5 μg

of the myc-tagged receptors (to attain equivalent receptor expression), 2.5 μg of dynamin-K44A, and 0.5 μg of FLAG-arrestin-3. This amount of FLAG-arrestin-3 was chosen because it gives an easily measurable signal but is lower than that required to attain half-maximal saturation as discussed above. Figure 2 shows representative experiments in which the association of arrestin-3 was measured with rLHR, hLHR, and exchange mutants thereof or rFSHR, hFSHR, and exchange mutants thereof. A quantitative assessment of the data obtained in several experiments is summarized in Figure 3. A quantitative comparison of the association of arrestin-3 with hLHR, rLHR, and their exchange mutants reveals a consistent correlation between the magnitude of arrestin-3 association and internalization. The large agonist-induced increase in arrestin-3 association with the hLHR correlates with a short half-time of internalization of hCG and a small agonist-induced increase in arrestin-3 association with the rLHR correlates with a long half-time of internalization of hCG (Figure 3A,B). Exchanging the seven residues highlighted in Figure 1 between the rLHR and hLHR lengthens the half-time of internalization of the hLHR to a value that approximates that of the rLHR and greatly reduces the agonist-induced increase in arrestin-3 association (Figure 3A). The complementary exchange shortens the half-time of internalization of the rLHR to a value that approximates that of the hLHR and greatly enhances the agonist-induced increase in arrestin-3 association (Figure 3B). A comparison of arrestin-3 association with the rFSHR (Figure 3C) and the hFSHR (Figure 3D) also reveals a similar inverse relationship. The short half-time of internalization of hFSH mediated by the rFSHR is accompanied by a large increase in agonist-induced arrestin-3 association, whereas the long half-time of internalization of the hFSHR is accompanied by a smaller agonist-induced increase in arrestin-3 association (Figure 3C,D). These data also show that exchanging the six rFSHR residues for the six hFSHR residues that lengthen the half-time of internalization of the rFSHR results in a reduction in arrestin-3 association, whereas exchanging the six hFSHR residues for the six rFSHR residues that shorten the half-time of internalization of the rLHR results in an enhancement of arrestin-3 association.

The seven LHR and six FSHR residues that control the rates of internalization and the extent of arrestin-3 association are present in three distinct regions: iL2, iL3, and the juxtamembrane region of the C-terminal tail of the LHR and TM4, iL3, and TM7 of the FSHR (see Figure 1). Since the relative importance of each of these regions to the process of internalization has already been evaluated by use of mutants containing complementary progressive substitutions of each receptor pair (*7*, *13*), the same mutants were used to evaluate the involvement of these residues on arrestin-3 association. Instead of using all complementary exchange constructs (as done in Figures 2 and 3), these experiments were done only with hLHR constructs with substituted rLHR residues and rFSHR constructs with substituted hFSHR residues because these are the constructs that display the greatest changes in arrestin-3 association (cf. Figure 3A,C). The data for the different hLHR constructs are presented in Figure 4 and show that substitution of the two divergent residues in iL2 and the single divergent residue in the C-terminal tail of the hLHR for the corresponding rLHR residues had little or no effect on arrestin-3 association, but

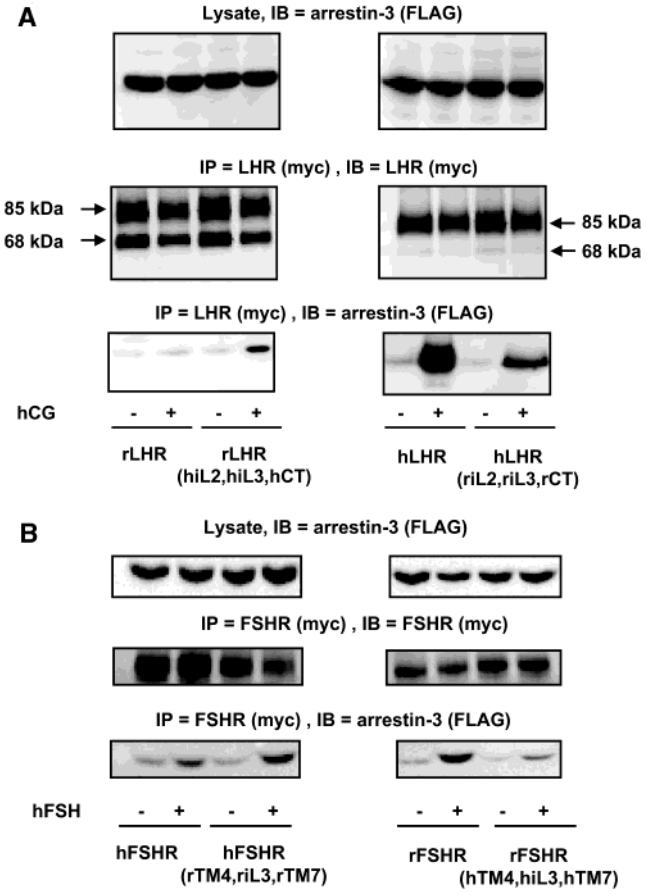

FIGURE 2: Association of FLAG-arrestin-3 with different LHR and FSHR constructs. 293T cells were plated in 100-mm dishes and cotransfected with FLAG-arrestin-3 (0.5 μg of plasmid), dynamin-K44A (2.5 μg of plasmid), and the indicated myc-tagged receptors (5 μg of plasmid). The cells were incubated without or with agonist (26 nM hCG for the LHR-transfected cells or 50 nM hFSH for the FSHR-transfected cells) at 37 °C for 30 min prior to cross-linking and immunoprecipitation as described under Materials and Methods. The results presented show the relevant areas of the blots of a representative experiment in which aliquots of the different lysates ($\sim$18 μL for the lysate blots and $\sim$500 μL for the blots of the immunoprecipitates) were used to measure the total amount of FLAG-arrestin-3 expressed in the lysate or the amount of myc-tagged receptor or FLAG-arrestin-3 immunoprecipitated with the 9E10 monoclonal antibody as described under Materials and Methods. In panel A, the 85 and 68 kDa bands shown in the myc blots of the myc immunoprecipitates represent the mature and immature forms of the LHR, respectively. As discussed elsewhere (see ref *43*), the immature form of the LHR is much more prominent in cells transfected with the rLHR than with the hLHR. In panel A, rLHR(hiL2,hiL3,hCT) refers to a rLHR mutant in which the two divergent residues in iL2, the four divergent residues in iL3, and the single divergent residue in the juxtamembrane region of the C-terminal tail were exchanged for the corresponding hLHR residues, whereas hLHR(riL2,riL3,rCT) refers to a hLHR mutant in which the two divergent residues in iL2, the four divergent residues in iL3, and the single divergent residue in the juxtamembrane region of the C-terminal tail were exchanged for the corresponding rLHR residues (see Figure 1 for the identity of these residues). In panel B, hFSHR(rTM4,riL3,rTM7) refers to a hFSHR mutant in which the two divergent residues in TM4, the three divergent residues in iL3, and the single divergent residue in TM7 were exchanged for the corresponding rFSHR residues, whereas rFSHR(hTM4,hiL3,hTM7) refers to a rFSHR mutant in which the two divergent residues in TM4, the three divergent residues in iL3, and the single divergent residue in TM7 were exchanged for the corresponding hFSHR residues (see Figure 1 for the identity of these residues). IP = immunoprecipitate, IB = immunoblot.

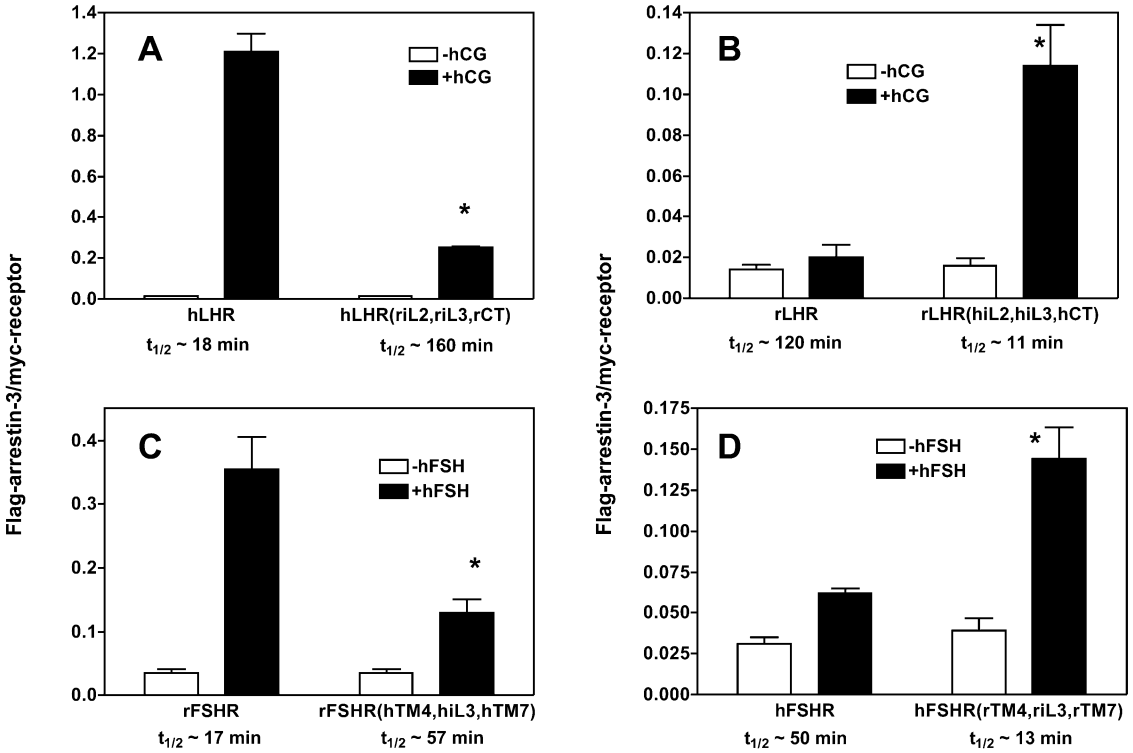

FIGURE 3: Quantitation of the association of FLAG-arrestin-3 with the human and rat gonadotropin receptors and mutants thereof. The association of arrestin-3 with the indicated receptors was measured as described in the caption for Figure 2 and under Materials and Methods. The amounts of FLAG-arrestin-3 and myc-tagged receptor present in the immunoprecipitates were quantitated as described under Materials and Methods, and the amount of receptor-associated arrestin-3 was calculated as the ratio of these two measurements. This ratio was plotted for each receptor pair as shown. The identity of the residues mutated in each of the constructs shown can be found in Figure 1. The approximate half-times of internalization of agonist mediated by each construct were measured in cells transfected only with the indicated receptor constructs and are shown under the appropriate bars. These values are taken from refs *7* and *8*. Each bar represent the mean (±SEM) obtained from 3−5 independent transfections. Asterisks denote statistically significant differences ($p < 0.05$) when compared to the corresponding wt receptor. Note the different scales among the different panels.

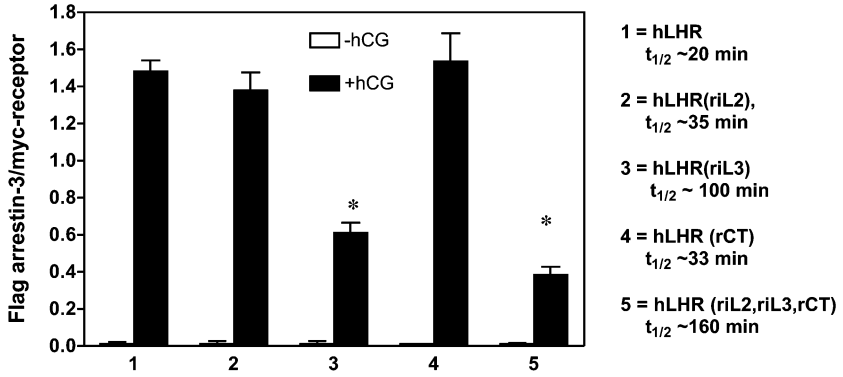

FIGURE 4: Quantitation of the association of FLAG-arrestin-3 with myc-hLHR constructs containing rLHR residue substitutions. 293T cells were plated in 100-mm dishes and cotransfected with FLAG-arrestin-3 (0.5 μg of plasmid), dynamin-K44A (2.5 μg of plasmid) and the indicated myc-tagged receptors (5 μg of plasmid). The cotransfected cells were incubated with (26 nM) or without hCG at 37 °C for 30 min prior to cross-linking and immunoprecipitation. The amounts of FLAG-arrestin-3 and myc-tagged receptor present in the immunoprecipitates were quantitated as described for Figure 2 and under Materials and Methods, and the amount of receptor-associated arrestin-3 was calculated as the ratio of these two measurements. This ratio was plotted for each receptor construct as shown. The approximate half-times of internalization of agonist mediated by each construct were measured in cells transfected only with the indicated receptor constructs and are shown under the appropriate bars. These values are taken from ref *7*. hLHR(ri2L) refers to a hLHR mutant in which the two divergent residues in iL2 were exchanged for the corresponding rLHR residues; hLHR(ri3L) refers to a hLHR mutant in which the four divergent residues in iL3 were exchanged for the corresponding rLHR residues; hLHR(rCT) refers to a hLHR mutant in which the single divergent residue in the juxtamembrane region of the C-terminal tail was exchanged for the corresponding rLHR residue; and hLHR-(riL2,riL3,rCT) refers to a hLHR mutant in which the two divergent residues in iL2, the four divergent residues in iL3, and the single divergent residue in the juxtamembrane region of the C-terminal tail were exchanged for the corresponding rLHR residues. The identity of the residues mutated is shown in Figure 1. Each bar represent the mean (±SEM) obtained from 3−5 independent transfections. Asterisks denote statistically significant differences ($p < 0.05$) when compared to the hLHR-wt.

substitution of the four divergent residues in iL3 decreased the agonist-induced arrestin-3 association. The magnitude of the reduction in arrestin-3 association detected with the iL3 exchange mutant is somewhat lower than that detected in the construct in which the iL2, iL3, and C-terminal tail residues were simultaneously mutated, however. A com-

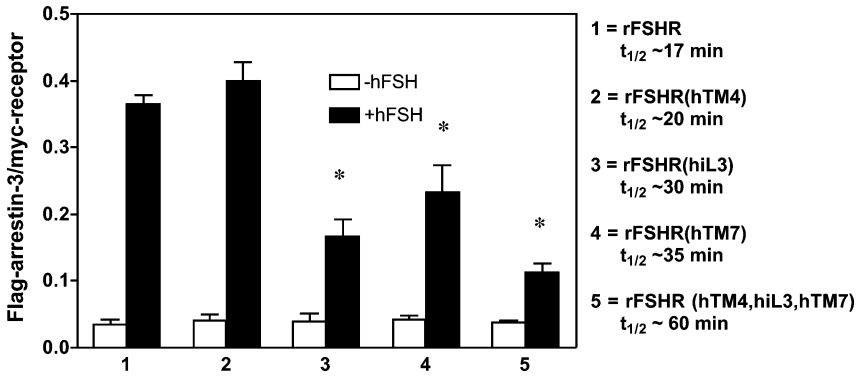

FIGURE 5: Quantitation of the association of arrestin-3 with myc-rFSHR constructs containing hFSHR residue substitutions. 293T cells were plated in 100-mm dishes and cotransfected with FLAG-arrestin-3 (0.5 μg of plasmid), dynamin-K44A (2.5 μg of plasmid), and the indicated myc-tagged receptors (5 μg of plasmid). The cotransfected cells were incubated with (50 nM) or without hFSH at 37 °C for 30 min prior to cross-linking and immunoprecipitation. The amounts of FLAG-arrestin-3 and myc-tagged receptor present in the immunoprecipitates were quantitated as described for Figure 2 and under Materials and Methods, and the amount of receptor-associated arrestin-3 was calculated as the ratio of these two measurements. This ratio was plotted for each receptor construct as shown. The approximate half-times of internalization of agonist mediated by each construct were measured in cells transfected only with the indicated receptor constructs and are shown under the appropriate bars. These values are taken from ref *8*. rFSHR(hTM4) refers to a rFSHR mutant in which the two divergent residues in TM4 were exchanged for the corresponding hFSHR residues; rFSHR(hiL3) refers to a rFSHR mutant in which the three divergent residues in iL3 were exchanged for the corresponding hFSHR residues; rFSHR(TM7) refers to a rFSHR mutant in which the two divergent residues in TM7 were exchanged for the corresponding hFSHR residues; and rFSHR(hTM4,hiL3,hTM7) refers to a rFSHR mutant in which the two divergent residues in TM4, the three divergent residues in iL3, and the two divergent residues in TM7 were exchanged for the corresponding hFSHR residues. The identity of the residues mutated is shown in Figure 1. Each bar represent the mean (±SEM) obtained from 3−5 independent transfections. Asterisks denote statistically significant differences ($p < 0.05$) when compared to the rFSHR-wt.

parison of the arrestin-3 association data with the half-times of internalization of hCG mediated by each of these mutants (Figure 4) revealed that the lack of effect of the iL2 and C-terminal tail exchange mutants on arrestin-3 association are associated with small changes (i.e., ≤2-fold) in the half-time of internalization, whereas the significant reduction in arrestin-3 association detected with the iL3 exchange mutant is associated with a more pronounced change in the half-time of internalization (i.e., ∼5-fold).

The data for the different rFSHR constructs are shown in Figure 5 and show that substitution of the two divergent residues in TM4 had no effect on arrestin-3 association whereas the substitution of the three divergent residues in iL3 or the single divergent residue in TM7 of the rFSHR impaired the agonist-promoted increase in arrestin-3 association. These changes correlate well with the effects of these mutations on the internalization of hFSH (Figure 5). The magnitude of the changes in internalization and arrestin-3 association observed with mutations of each region is somewhat lower than that detected in the rFSHR construct in which the TM4, iL3, and TM7 residues were simultaneously mutated (Figure 5).

The TM7 residues of the FSHR (His in the hFSHR and Tyr in the rFSHR; see Figure 1) that were shown to influence arrestin-3 association and internalization have been recently implicated as being involved in interhelical hydrophobic interactions that stabilize the activated/inactivated states of the FSHR (*26*). Since it is likely that the effects of this residue on arrestin-3 association are indirectly mediated by changes in conformation of the intracellular loops rather than by a direct interaction of this residue with arrestin-3, its potential importance on the formation of the FSHR/arrestin-3 complex was not investigated further. On the other hand, since our data show that iL3 is the only region that affects the formation of the receptor/arrestin-3 complex and internalization on each of the two gonadotropin receptor pairs, we performed additional experiments designed to define which iL3 residues are responsible for these effects.

The three divergent iL3 residues of the rFSHR (Thr^{532}, Thr^{542}, and Lys^{551}) were mutated to the corresponding hFSHR residues (Ile, Asn, and Arg, respectively; see Figure 1) and the functional properties of these mutants were compared to those of the mutant in which all three residues were simultaneously exchanged. These data are presented in Table 1 and show that the individual substitution of each rFSHR residue for the corresponding hFSHR residue impairs the association of arrestin-3 with the rFSHR to about the same extent as when all residues are simultaneously substituted [i.e., the rFSHR(hiL3) construct]. Only two of these three residues (Thr^{532} and Thr^{542}), however, contribute to the difference in the rate of internalization between the rFSHR and hFSHR. Since the rFSHR is known to be phosphorylated on Ser and Thr residues present in iL3 (*27*, *28*) but the formation of the arrestin-3/rFSHR complex occurs independently of the phosphorylation of these residues (*14*), we also tested the effects of additional mutations of Thr^{532} and Thr^{542} on the formation of the arrestin-3/rFSHR complex and the internalization of hFSH. These two residues were individually mutated to Ala (a non-phosphate acceptor), Ser (another phosphate acceptor), or Asp (which should mimic the charge of a phosphorylated residue). The results of these experiments are also summarized in Table 1 and show that mutation of T^{532} to Ala, Ser, or Asp had no effect on the association of the rFSHR with arrestin-3 or on the half-time of internalization of hFSH. In contrast, mutation of T^{542} to Ala, Ser, or Asp significantly reduced the association of the rFSHR with arrestin-3 and lengthened the half-time of internalization of hFSH.

The discrepancy between the effects of the K551R mutation of the rFSHR on arrestin-3 association and internalization is puzzling and remains unresolved. It is worth

Table 1: Mutations of Selected Third Intracellular Loop Residues of the FSHR Affect the Formation of the rFSHR/Arrestin-3 Complex and the Internalization of hFSH[a]

rFSHR	receptor-associated arrestin-3 (*x*-fold over basal)	hFSH internalization $t_{1/2}$ (min)
wt	26 ± 5	16 ± 1
hiL3[b]	10 ± 3[c]	30 ± 3[c]
T532I	7 ± 2[c]	34 ± 1[c]
T542N	5 ± 1[c]	33 ± 2[c]
K551R	11 ± 3[c]	15 ± 1
T532A	17 ± 2	15 ± 2
T532S	17 ± 6	20 ± 1
T532D	16 ± 3	19 ± 2
T542A	11 ± 3[c]	34 ± 1[c]
T542S	7 ± 1[c]	32 ± 5[c]
T542D	8 ± 1[c]	42 ± 5[c]

[a] For arrestin-3 binding assays, the cells were plated in 100-mm dishes and cotransfected with FLAG-arrestin-3 (0.5 μg), dynamin-K44A (2.5 μg), and the indicated myc-tagged receptor constructs (5 μg). The cells were then incubated with (50 nM) or without hFSH at 37 °C for 30 min and the association of arrestin-3 with the indicated constructs was measured as described in the caption for Figure 2 and under Materials and Methods. The amount of immunoprecipitated arrestin-3 was measured in control and stimulated cells and divided by the amount of receptor present in the immunoprecipitates. All data are expressed as x-fold over the amount of receptor-associated arrestin-3 present in unstimulated cells. For internalization assays, the cells were transfected only with the indicated receptor constructs and the half-time of internalization of ^{125}I-hFSH was measured as described under Materials and Methods. Each number represent the mean (±SEM) obtained from at least three independent transfections. [b] Note that rFSHR(hiL3) is a construct containing the T532I, T542N and K551R mutations. [c] Statistically significant differences ($p < 0.05$) when compared to the rFSHR-wt.

Table 2: Mutations of Selected Third Intracellular Loop Residues of the hLHR Affect the Formation of the hLHR/Arrestin-3 Complex and the Internalization of hCG[a]

hLHR	receptor-associated arrestin-3 (*x*-fold over basal)	hCG internalization $t_{1/2}$ (min)
wt	313 ± 76	20 ± 1
riL3[b]	113 ± 22[c]	109 ± 9[c]
K548R	367 ± 66	38 ± 3[c]
R554Q	327 ± 62	23 ± 4
M559T	240 ± 62	22 ±2
T561P	143 ± 27[c]	75 ± 5[c]
T561A	230 ± 25	22 ± 1
T561S	120 ± 46[c]	52 ± 3[c]
T561D	122 ± 22[c]	71 ± 8[c]

[a] For arrestin-3 binding assays, the cells were plated in 100-mm dishes and cotransfected with FLAG-arrestin-3 (0.5 μg), dynamin-K44A (2.5 μg), and the indicated myc-tagged receptor constructs (5 μg). The cells were then incubated with (26 nM) or without hCG at 37 °C for 30 min and the association of arrestin-3 with the indicated constructs was measured as described in the captions for Figures 2−4 and under Materials and Methods. The amount of immunoprecipitated arrestin-3 was measured in control and stimulated cells and divided by the amount of receptor present in the immunoprecipitates. All data were expressed as *x*-fold over the amount of receptor-associated arrestin-3 present in unstimulated cells. For internalization assays, the cells were transfected only with the indicated receptor constructs and the half-time of internalization of ^{125}I-hCG was measured as described under Materials and Methods. Each number represent the mean (±SEM) obtained from at least three independent transfections. [b] Note that hLHR(riL3) is a construct containing the K548R, R554Q, M559T and T561P mutations. [c] Statistically significant differences ($p < 0.05$) when compared to the hLHR-wt.

mentioning, however, that of 28 mutants analyzed in this paper, this is the only mutant that displayed a significant reduction in arrestin-3 association that was not accompanied by a significant change in the half-time of internalization. The opposite is not true, however, as there are three examples of mutants [hLRH(riL2), hLHR(rCT) and hLHR-K548R] that display changes in internalization that are not accompanied by changes in arrestin-3 association (cf. Figure 4 and Table 2). This is probably due to the greater sensitivity of the internalization assay as compared to that of the arrestin-3 association assay.

Similar experiments were performed by mutating the four divergent iL3 residues of the hLHR (Lys^{548}, Arg^{554}, Met^{559}, and Thr^{561}) to the corresponding rLHR residues (Arg, Gln, Thr, and Pro, respectively; see Figure 1) and the functional properties of each of these mutants were compared to those of the hLHR(riL3) construct in which all four iL3 residues were simultaneously mutated to those present in the rLHR. These results are presented in Table 2 and show that the differences in arrestin-3 association and the half-times of internalization of hCG are due mostly to the presence of a Thr in the hLHR or a Pro in the rLHR at the position equivalent to codon 561 of the hLHR. To complement the experiments done with the rFSHR (see Table 1), the functional properties of hLHR mutants in which Thr^{561} was mutated to Ala, Ser, or Asp were also examined. These results are also presented in Table 2 and show that a T561A mutation has no significant effect on arrestin-3 association or hCG internalization, whereas the T561S and T561D mutations reduce arrestin-3 association and lengthen the half-time of internalization of hCG to about the same extent as the T561P mutation.

Collectively, the data presented in Tables 1 and 2 highlight the importance of the T532I and T542N exchange mutants of the FSH receptors and the T561P exchange mutant of the LH receptors in arrestin-3 association and ligand internalization.

Since the arrestin-3 association assays were done in cells cotransfected with a small amount of arrestin-3 but the internalization assays were done in cells that were not cotransfected with arrestin-3, it was important to ascertain that the reported changes in internalization could be detected in cells cotransfected with arrestin-3. Thus, additional internalization assays were performed with rFSHR-wt, rFSHR-T532I, and rFSHR-T542N (Figure 6A) as well as with the hLHR-wt and the hLHR-T561P mutant (Figure 6B) in cells cotransfected with increasing amounts of arrestin-3 plasmid. In the case of the rFSHR-T542N (Figure 6A) or hLHR-T561P (Figure 6B) mutants, a slow rate of internalization was detected in cells cotransfected with up to 10 μg of arrestin-3 plasmid/100-mm dish. The slower rate of internalization of the rFSHR-T532I mutant was also preserved in cells cotransfected with the lower amounts of arrestin-3 plasmid used in the arrestin-3 association assays but it was rescued in cells cotransfected with high amounts of arrestin-3 plasmid (Figure 6A). When assayed in cell expressing increasing amounts of arrestin-3, the rates of internalization of hCG or hFSH by the four parent chimeras shown in Figures 2 and 3 herein are similar to that of the rFSHR-T532I mutant (*7*, *8*).

Finally, because the association of GPCRs with the nonvisual arrestins is also dependent on receptor activation,

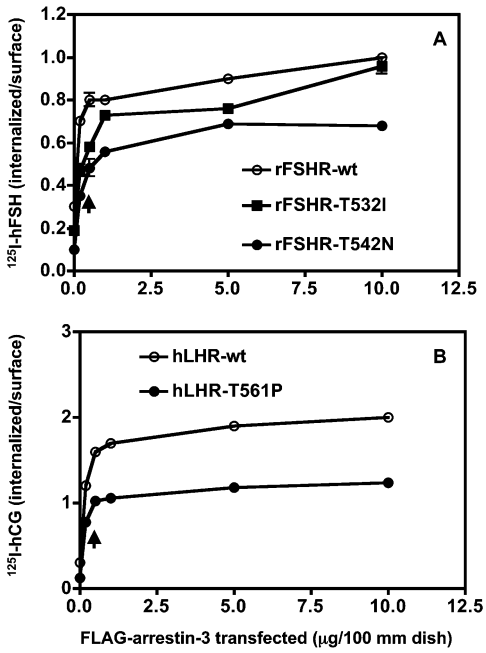

FIGURE 6: Effects of increasing amounts of arrestin-3 on the internalization of gonadotropins mediated by myc-rFSHR-wt, myc-hLHR-wt, and mutants thereof. The internalization of ^{125}I-hFSH (panel A) or ^{125}I-hCG (panel B) was measured in 293T cells cotransected with a constant amount of myc-tagged receptor plasmid (5 μg/100-mm dish) and increasing amounts of FLAG-arrestin-3 as indicated. The amount of surface-bound and internalized ^{125}I-hCG were determined during a 10 min incubation of the transfected cells with 2 nM ^{125}I-hFSH (panel A) or ^{125}I-hCG (panel B) as described under Materials and Methods and plotted as a function of the amount of FLAG-arrestin-3 transfected. Each point shows the average ± SEM of three independent transfections. Some error bars are not visible because they fall within the symbols. The arrows indicate the amount of FLAG-arrestin-3 used to transfect cells for the arrestin-3 association assays.

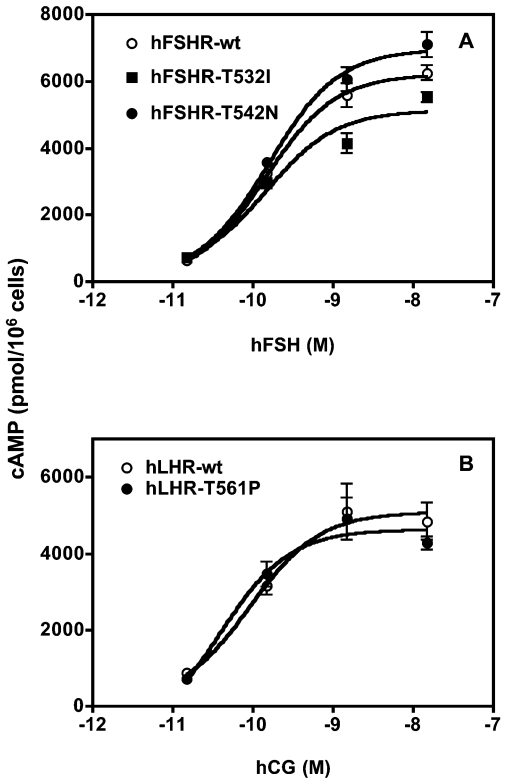

FIGURE 7: Signaling properties of myc-rFSHR-wt, myc-hLHR-wt, and mutants thereof. 293T cells were plated in 35-mm wells and transected with 1 μg of the indicated plasmids to attain equivalent receptor expression. The cells were then incubated with increasing concentrations of hFSH (panel A) or hCG (panel B) for 2 h at 37 °C and the amount of cAMP accumulated was measured as described under Materials and Methods. Each point shows the average ± SEM of three independent transfections.

it was important to determine if the exchange mutants described above display a reduction in agonist-induced receptor activation. The results summarized in Figure 7 and Table 3 show that the ability of hFSH to simulate cAMP accumulation in cells expressing the rFSHR-T532I and rFSHR-T542N mutants is very similar to that displayed by cells expressing the rFSHR-wt. Similarly, the dose−response curves for the hCG-induced increase in cAMP accumulation are very similar to the curves for the hLHR-wt and the hLHR-T561P mutant. These results are not surprising because the mutants in question were designed on the basis of the amino acid sequences of the gonadotropin receptors from different mammalian species. Moreover, the four parent chimeras shown in Figures 2 and 3 have already been shown to respond normally to gonadotropin stimulation (*7*, *8*).

Table 3: Ligand Binding and Signaling Properties of Selected hLHR and rFSHR Mutants[a]

receptor	hormone bound (fmol/10^6 cells)	EC_{50} (M)	maximal response (pmol of cAMP/10^6 cells)
rFSHR-wt	87 ± 2	1.4 (± 0.01) × 10^{-10}	6217 ± 41
rFSHR-T532I	84 ± 1	1.4 (± 0.03) × 10^{-10}	5133 ± 209
rFSHR-T542N	84 ± 2	1.6 (± 0.01) × 10^{-10}	6967 ± 96
hLHR-wt	123 ± 7	0.9 (± 0.02) × 10^{-10}	5090 ± 96
hLHR-T561P	118 ± 8	0.8 (± 0.02) × 10^{-10}	4634 ± 142

[a] Hormone binding was measured during a 1 h incubation of intact cells with a saturating concentration (~50 nM) of ^{125}I-hFSH or ^{125}I-hCG to intact cells as described in refs 7 and 8. Maximal cAMP responses and EC_{50}s were calculated from the dose−response curves shown in Figure 7 as described under Materials and Methods. The numbers shown are the mean ± SEM of three independent transfections.

DISCUSSION

Since the internalization of many GPCRs is driven by their interaction with the nonvisual arrestins, we reasoned that a mutagenesis approach that used internalization assays as readout would result in the identification of GPCR residues that participate in the formation of the GPCR/nonvisual arrestin complex. To this end, we first took advantage of the different rates of internalization of the LHR and FSHR derived from rats and humans and a complementary exchange mutagenesis approach to identify a limited number of divergent, noncontiguous residues (six for the FSHR and seven for the LHR) present in the serpentine and C-terminal domains of these receptors that are responsible for their divergent rates of internalization (Figure 1 and refs *7* and *8*). The new studies presented here show that the divergent rates of internalization of these two pairs of gonadotropin receptors correlate with differences in their abilities to associate with arrestin-3 and that the divergent residues that dictate internalization also dictate the ability of these receptors to associate with arrestin-3 (Figures 2−5). Thus, the mutagenesis/internalization approach is powerful and useful in the identification of GPCR residues that participate

in the formation of the GPCR/nonvisual arrestin complexes.

Although the seven divergent residues of the rLHR/hLHR and rFSHR/hFSHR pairs that dictate their rates of internalization are present in distinct topological domains (Figure 1), iL3 is the only common region between the two pairs of gonadotropin receptors that affects internalization and arrestin-3 binding. This finding is interesting because previous studies have implicated iL3 as being important for the interaction of several GPCRs (*29*, *30*), including the LHR (*31*, *32*) with arrestins. Since those studies were done by measuring the binding of purified arrestins to isolated iL3 peptides or mutants thereof, they could not be used to ascertain the importance of iL3 relative to that of other GPCR regions in the formation of the arrestin/GPCR complex. Our studies, which were done with the intact gonadotropin receptors, are therefore unique and important because they highlight the importance of iL3 in the context of the full-length receptor. The only other study similar to ours was done by testing synthetic peptides derived from different regions of rhodopsin for their ability to inhibit the binding of arrestin-1 to light-activated, phosphorylated rhodopsin (*33*). The results of this study also highlighted the importance of iL3 in the formation of the rhodopsin/arrestin-1 complex (*33*). The finding that our unbiased approach resulted in the identification of residues present in iL3 as being involved in the interaction of the gonadotropin receptors with arrestin-3 is also noteworthy because this region is particularly important in the agonist-induced recognition and activation of G proteins by GPCRs (*34*−*37*).

Although the amino acid sequences of the third intracellular loops of the LHR and FSHR are not particularly conserved (Figure 1), we found that the identity of the 3iL residues that contribute to arrestin-3 association is indeed conserved. Thr^{542} in the 3iL of the rFSHR and Thr^{561} in the 3iL of the hLHR are particularly important for the formation of the receptor/arrestin-3 complex (Tables 1 and 2). Like many other GPCRs, the formation of the rFSHR/arrestin-3 complex is dependent upon the activation and the phosphorylation of the FSHR (*14*). Although serine and threonine residues present in iL3 of the rFSHR become phosphorylated upon hFSH binding (*27*, *28*, *38*), the mutagenesis studies presented here (Table 1) suggest that the phosphorylation of Thr^{532} and/or Thr^{542} of the rFSHR are not needed for the formation of the FSHR/arrestin-3 complex. In contrast, the formation of the hLHR/arrestin-3 complex is not dependent on the phosphorylation of the hLHR (*12*) and the agonist-induced phosphorylation of this receptor maps to serine residues present in its C-terminal tail (*11*, *16*). In agreement with these observations, the mutagenesis studies done with the hLHR also indicate that the phosphorylation of Thr^{561} is not needed for the formation of the LHR/arrestin-3 complex. In fact, the mutagenesis studies (Table 1) indicate that the presence of a threonine residue at position 542 in iL3 of the rFSHR is optimal for arrestin-3 association because the mutation of this residue to four other amino acids (Asn, Ala, Ser, or Glu) impairs the formation of the FSHR/arrestin-3 complex. A different conclusion can be drawn about the role of Thr^{532}, however. In this case only a Thr to Ile mutation reduced arrestin-3 association whereas mutations to Ala, Ser, or Asp had no effect. Therefore, the presence of Ile in the equivalent position of the hFSHR appears to be responsible for the reduced association of this receptor with arrestin-3. Thr^{561} in iL3 of the hLHR also appears to promote arrestin-3 association because the mutation of this residue to Pro (the equivalent residue in the rLHR), Ser, or Asp impaired the formation of the LHR/arrestin-3 complex (Table 2). A substitution of this residue for Ala is permissible, however, as it has no effect on arrestin-3 association (Table 2).

A number of recent studies measuring the binding of nonvisual arrestins to iL3 peptides of the different subtypes of α2-adrenergic receptors (*30*) and the LHR (*31*, *32*) suggest that basic residues present in iL3 of GPCRs are essential for the binding of nonvisual arrestins. It is interesting to note that one of the three divergent residues in iL3 of the rFSHR/hFSHR pair is basic but conservatively substituted (K551R; see Table 1). As already discussed above, this residue appears to have an effect on arrestin-3 association but not on internalization. Two of the four divergent residues in iL3 of the rLHR/hLHR pair are also basic but only one is conservatively substituted (K548R; see Table 2) while the other is not (R554Q; see Table 2). Neither of these two seems to have a major effect on the association of the hLHR with arrestin-3, however. When assayed in vitro by a synthetic peptide approach, Asp^{564} in iL3 of the hLHR was shown to be essential for the binding of arrestin-2 (*32*). The importance of this residue was not investigated here because it is conserved between the rLHR and the hLHR (cf. Figure 1). Finally, as already noted above, other investigators have been able to detect high-affinity ($K_d \sim 100$ pM) binding of purified arrestin-2 to synthetic peptides corresponding to the third intracellular loop of the LHR (*31*, *32*). Curiously, however, the binding of purified arrestin-3 to these peptides was undetectable (*32*).[3]

[3] We have also been unable to reliably detect binding of arrestin-3 to the third intracellular loop of the hLHR or the rFSHR expressed as GST fusion proteins.

ACKNOWLEDGMENT

We thank Dr. Deborah Segaloff for a critical reading of the manuscript. We also thank Dr. Jeff Benovic (Thomas Jefferson University, Philadephia, PA) for the original arrestin-3 construct, Dr. Sandra Schmid (Scripps Research Institute, La Jolla, CA) for the HA-tagged dynamin K44A construct, and Dr. Marlene Hosey (Northwestern University, Chicago, IL) for human kidney 293T cells. We also thank Ares Serono (Randolph, MA) for the original human LHR construct and for recombinant hCG.

REFERENCES

1. Perry, S. J., and Lefkowitz, R. J. (2002) *Trends Cell Biol. 12*, 130−138.
2. Luttrell, L. M., and Lefkowitz, R. J. (2002) *J. Cell. Sci. 115*, 455−465.
3. Kim, Y.-M., and Benovic, J. L. (2002) *J. Biol. Chem. 277*, 30760−30768.
4. Pan, L., Gurevich, E. V., and Gurevich, V. V. (2003) *J. Biol. Chem. 278*, 11623−11632.
5. Laporte, S. A., Miller, W. E., Kim, K.-M., and Caron, M. G. (2002) *J. Biol. Chem. 277*, 9247−9254.
6. Nakamura, K., Liu, X., and Ascoli, M. (1999) *J. Biol. Chem. 274*, 25426−25432.
7. Nakamura, K., Liu, X., and Ascoli, M. (2000) *J. Biol. Chem. 275*, 241−247.
8. Kishi, H., and Ascoli, M. (2000) *J. Biol. Chem. 275*, 31030−31037.

9. Kishi, M., Liu, X., Hirakawa, T., Reczek, D., Bretscher, A., and Ascoli, M. (2001) *Mol. Endocrinol. 15*, 1624−1635.
10. Baratti-Elbaz, C., Chinea, N., Lahuna, O., Loosfelt, H., Pichon, C., and Milgrom, E. (1999) *Mol. Endocrinol. 13*, 1751−1765.
11. Galet, C., Min, L., Narayanan, R., Kishi, M., Weigel, N. L., and Ascoli, M. (2003) *Mol. Endocrinol. 17*, 411−422.
12. Min, L., Galet, C., and Ascoli, M. (2002) *J. Biol. Chem. 277*, 702−710.
13. Kishi, H., Krishnamurthy, H., Galet, C., Bhaskaran, R. S., and Ascoli, M. (2002) *J. Biol. Chem. 277*, 21939−21946.
14. Krishnamurthy, H., Galet, C., and Ascoli, M. (2003) *Mol. Cell. Endocrinol. 204*, 127−140.
15. Fabritz, J., Ryan, S., and Ascoli, M. (1998) *Biochemistry 37*, 664−672.
16. Min, L., and Ascoli, M. (2000) *Mol. Endocrinol. 14*, 1797−1810.
17. Damke, H., Baba, T., Warnock, D. E., and Schmid, S. L. (1994) *J. Cell Biol. 127*, 915−934.
18. Chen, C., and Okayama, H. (1987) *Mol. Cell. Biol. 7*, 2745−2752.
19. Quintana, J., Hipkin, R. W., and Ascoli, M. (1993) *Endocrinology 133*, 2098−2104.
20. Wiley, H. S., and Cunningham, D. D. (1981) *Cell 25*, 433−440.
21. Wiley, H. S., and Cunningham, D. D. (1982) *J. Biol. Chem. 257*, 4222−4229.
22. Lloyd, C. E., and Ascoli, M. (1983) *J. Cell Biol. 96*, 521−526.
23. Ascoli, M., and Segaloff, D. L. (1987) *Endocrinology 120*, 1161−1172.
24. Margolskee, R., McHenry-Rinde, B., and Horn, R. (1993) *BioTechniques 15*, 906−911.
25. Qian, H., Pipolo, L., and Thomas, W. G. (2001) *Mol. Endocrinol. 15*, 1706−1719.
26. Tao, Y.-X., Mizrachi, D., and Segaloff, D. L. (2002) *Mol. Endocrinol. 16*, 1881−1892.
27. Nakamura, K., Hipkin, R. W., and Ascoli, M. (1998) *Mol. Endocrinol. 12*, 580−591.
28. Nakamura, K., Krupnick, J. G., Benovic, J. L., and Ascoli, M. (1998) *J. Biol. Chem. 273*, 24346−24354.
29. Wu, G., Krupnick, J., Benovic, J., and Lanier, S. (1997) *J. Biol. Chem. 272*, 17836−17842.
30. DeGraff, J. L., Gurevich, V. V., and Benovic, J. L. (2002) *J. Biol. Chem. 277*, 43247−43252.
31. Mukherjee, S., Palczewski, K., Gurevich, V. V., and Hunzicker-Dunn, M. (1999) *J. Biol. Chem. 274*, 12984−12989.
32. Mukherjee, S., Gurevich, V. V., Preninger, A., Hamm, H. E., Bader, M.-F., Fazleabas, A. T., Birnbaumer, L., and Hunzicker-Dunn, M. (2002) *J. Biol. Chem. 277*, 17916−17927.
33. Krupnick, J. G., Gurevich, V. V., Shepers, T., Hamm, H. E., and Benovic, J. L. (1994) *J. Biol. Chem. 269*, 3226−3232.
34. Liggett, S. B., Caron, M. G., Lefkowitz, R. J., and Hnatowich, M. (1991) *J. Biol. Chem. 266*, 4816−4821.
35. Greasley, P. J., Fanelli, F., Scheer, A., Abuin, L., Nenniger-Tosato, M., DeBenedetti, P. G., and Cotecchia, S. (2001) *J. Biol. Chem. 276*, 46485−46494.
36. Wang, H., Jaquette, J., Collison, K., and Segaloff, D. L. (1993) *Mol. Endocrinol. 7*, 1437−1444.
37. Shulz, A., Schöneberg, T., Paschke, R., Schultz, G., and Gudermann, T. (1999) *Mol. Endocrinol. 13*, 181−190.
38. Hipkin, R. W., Liu, X., and Ascoli, M. (1995) *J. Biol. Chem. 270*, 26683−26689.
39. Sprengel, R., Braun, T., Nikolics, K., Segaloff, D. L., and Seeburg, P. H. (1990) *Mol. Endocrinol. 4*, 525−530.
40. Minegishi, T., Nakamura, K., Takakura, Y., Ibuki, Y., and Igarashi, M. (1991) *Biochem. Biophys. Res. Commun. 175*, 1125−1130.
41. McFarland, K. C., Sprengel, R., Phillips, H. S., Kohler, M., Rosemblit, N., Nikolics, K., Segaloff, D. L., and Seeburg, P. H. (1989) *Science 245*, 494−499.
42. Minegishi, T., Nakamura, K., Takakura, Y., Miyamoto, K., Hasegawa, Y., Ibuki, Y., and Igarashi, M. (1990) *Biochem. Biophys. Res. Commun. 172*, 1049−1054.
43. Ascoli, M., Fanelli, F., and Segaloff, D. L. (2002) *Endocrine Rev. 23*, 141−174.

BI034907W